J. Fluid Mech. (2001), *vol.* 439, *pp.* 199–216. Printed in the United Kingdom

A solution technique for longitudinal Stokes flow around multiple aligned cylinders

By S. TOLL

Chalmers University of Technology, Department of Polymeric Materials,
SE-41296 Göteborg, Sweden

(Received 13 September 2000 and in revised form 3 January 2001)

This technique solves the two-dimensional Poisson equations in geometries involving cylindrical objects. The method uses three fundamental solutions, corresponding to a line force, a line couple and a pressure gradient, on each cylinder. Superposition of the fundamental solutions due to all the cylinders involved, while approximately satisfying the no-slip condition on each cylinder, yields a mobility matrix relating the various forces and motions of all the cylinders. Any specific problem can be solved by prescribing the motions of the cylinders and solving the matrix. For problems involving few cylinders or with a sufficient degree of symmetry this can be done analytically.

Once constructed, the general method is applied analytically to a series of specific problems. The permeability of an eccentric annulus is derived. The result is numerically indistinguishable from the exact solution to the problem, but unlike the exact solution the present one is obtained in closed form. The drag on two parallel rods moving past one another is also derived and compared to the exact solution. In this case the result is accurate for rod separations down to about 0.2 times the rod diameter. Finally the drag on a rod moving in a triangular array of identical rods is derived. Here it is shown that due to screening it is sufficient to include the six nearest neighbours, regardless of the rod separation. Although the present examples are all worked out analytically, the matrix can also be solved numerically, in which case any two-dimensional arrangement of cylindrical objects can be studied.

1. Introduction

Consider longitudinal steady-state viscous flow in a prismatic geometry consisting of a set of parallel infinitely long prismatic solid bodies. Such a flow involves no accelerations anywhere and hence no inertia. It is therefore governed by the two-dimensional Poisson equation,

$$\frac{\partial v^2}{\partial x^2} + \frac{\partial v^2}{\partial y^2} = \frac{1}{\mu}\frac{\partial P}{\partial z}, \tag{1}$$

where $v = v(x, y)$ is the longitudinal (z-parallel) fluid velocity and $\partial P/\partial z$ is the longitudinal pressure gradient. Any particular problem in this category is distinguished by the shape and position of the boundary curve of each body along with an auxiliary condition on each body, for example a prescribed motion or a prescribed resultant force or couple or any combination thereof. In particular, the pressure gradient may or may not vanish.

In practical problems, where bodies have finite length, equation (1) holds only

approximately. But the approximation will be good wherever the problem has this two-dimensional nature. This criterion will be satisfied at all points that are much nearer to a solid body than to the end of a body. At points close to the end of a body, the flow will be three-dimensional and may involve inertia. In the type of micromechanical problems considered below, such regions may be simply ignored provided that they constitute a negligible part of the overall volume. This leads to a condition of slenderness of the interstices,

$$H/L \ll 1, \tag{2}$$

where H is the interstitial spacing between two solid boundaries and L is the length of the bodies.

There are two important special cases of this type of problem. The first is the problem of estimating the longitudinal Darcy permeability of an array of fixed rods. Here the flow is driven entirely by the pressure gradient. Most of the work reported concerns infinite regular arrays of identical cylinders. The simplest approach seems to be the free-surface model by Happel (1959). Howells (1974) developed a self-consistent model in which distant particles are represented as a Darcy resistance while the nearest-neighbour interactions are solved explicitly. The best solution so far seems to be that published by Drummond & Tahir (1984) using Lord Rayleigh's (1892) method of singularities. Incidentally, they comment that Happel's simple cell model is fairly good at large rod separations.

The other case concerns estimating the hydrodynamic drag on a rod moving relative to a surrounding array of rods, such as in the elongational flow of a suspension of parallel fibres. In this case the pressure gradient vanishes and the flow is driven by the relative motion of the rods. The problem was first described by Batchelor (1971), who suggested a simple axisymmetric cell model, in a sense analogous to the Happel model, with a test rod at the centre and a concentric cylindrical boundary to represent the surrounding particles. Again, there is also a self-consistent model, suggested by Acrivos & Shaqfeh (1988), where a test particle is suspended in a liquid having the effective properties sought. The most rigorous analysis so far was presented by Shaqfeh & Fredrickson (1990), who solved the multi-body interactions by multiple scattering based on slender-body theory (Batchelor 1970). All these methods are reasonably good at sufficiently large rod separations, but none is accurate at small rod separations, say of the order of a rod radius or less. This is either because of ignoring the details of the fibre arrangement, as in the case of Bachelor's cell model or the self-consistent approach, or because of neglecting fluid couples on the particles, as in the case of slender-body theory. It should be mentioned that the method of Shaqfeh & Fredrickson applies to three-dimensional fibre arrangements, not just the parallel rods considered here. Simplified cell models are useful for modelling flows of non-Newtonian fluids (Goddard 1976; Pipes 1994), where they are often the only route possible.

It will be shown here that in the two-dimensional case of aligned cylinders it is quite possible to solve this type of problem accurately without simplifying the geometry. The objective of the analysis is to solve the many-body problem for a general array that is not restricted by symmetry conditions nor represented by any simplified cell boundary condition. We shall study the mixed resistance/mobility problem of N circular cylinders of different radii in a general array, each moving longitudinally at a prescribed axial velocity. Compared to the corresponding solution by the method of reflections, as suggested by Shaqfeh & Fredrickson, the main advantage of the

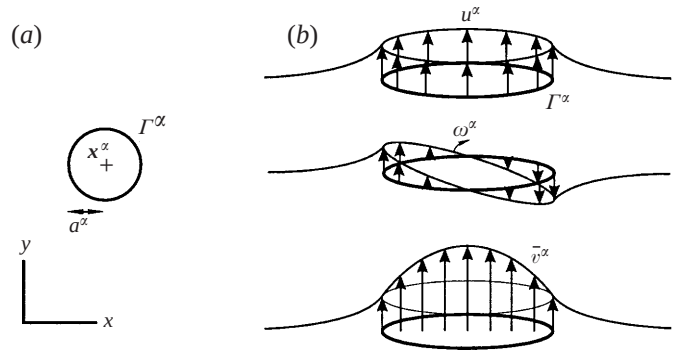

FIGURE 1. (*a*) Circular boundary; (*b*) motions.

present solution lies in the inclusion of fluid couples. This will allow particles to come considerably closer together.

When computing the drag on a test rod in an infinite array the question arises as to how many neighbouring rods need to be included in the model. Clearly, rods sufficiently far from the test rod do not contribute to the force on the test rod. This is sometimes referred to as *screening* and will be addressed here.

2. Mobility method

The solution scheme developed here is akin to Stokesian dynamics in two dimensions (Brady & Bossis 1988). A solution $v(\boldsymbol{x})$ for the two-dimensional velocity field will be constructed by superposition of a finite set of fundamental solutions, $v_{(\alpha)}(\boldsymbol{x})$, each of which matches a restricted motion and a particular moment of force on a circular boundary curve in the (x, y)-plane. The curves may be used to represent actual solid boundaries, in which case their motion should be interpreted as that of a solid body. However, they may also serve more general purposes, as I shall exemplify later.

As illustrated in figure 1, each circle Γ^α is assigned a centre $\boldsymbol{x}^\alpha$ and a radius a^α and is associated with four motions,

$$\boldsymbol{U}^\alpha = (u^\alpha, \omega_x^\alpha, \omega_y^\alpha, \bar{v}^\alpha), \tag{3}$$

where u^α is the linear z-velocity of Γ^α, ω_x^α and ω_y^α are angular velocities about the x- and y-axes and $\bar{v}^\alpha$ is the mean velocity within Γ^α, i.e.

$$\bar{v}^\alpha = \frac{1}{\pi(a^\alpha)^2} \int_{A^\alpha} v \, \mathrm{d}A. \tag{4}$$

Notice that all of these motions are purely longitudinal and preserve a circular cylindrical geometry; thus the angular motion is actually a motion of longitudinal shear. When the cylinders are used to model rigid bodies we must require the angular motions to vanish; nevertheless this motion is a necessary degree of freedom if we want to include fluid couples. Let $v_{(\alpha)}(\boldsymbol{x})$ be the fluid velocity field generated by the motion of a single boundary Γ^α. The exact solution $v_{(\alpha)}(\boldsymbol{x})$ consists of a sum of four fundamental solutions to the two-dimensional Poisson equations, each of which

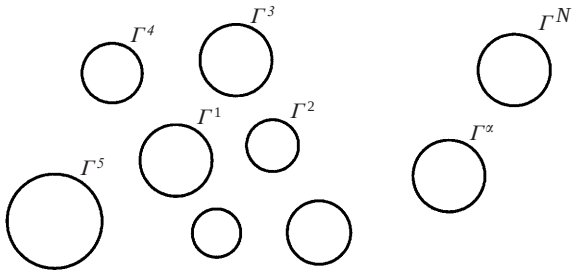

FIGURE 2. Boundary curves.

exactly matches one of the four motions:

$$v_{(\alpha)}(\boldsymbol{x}) = \begin{cases} \dfrac{1}{2\pi\mu}\left((f^\alpha + p^\alpha)\ln\dfrac{\rho}{|\boldsymbol{x}-\boldsymbol{x}^\alpha|} + l_x^\alpha\dfrac{y-y^\alpha}{|\boldsymbol{x}-\boldsymbol{x}^\alpha|^2} - l_y^\alpha\dfrac{x-x^\alpha}{|\boldsymbol{x}-\boldsymbol{x}^\alpha|^2}\right) & \\ \qquad\qquad\qquad\qquad\qquad\qquad\qquad\qquad \text{if} \quad |\boldsymbol{x}-\boldsymbol{x}^\alpha| \geqslant a^\alpha & \\ \dfrac{1}{2\pi\mu}\left((f^\alpha + p^\alpha)\ln\dfrac{\rho}{a^\alpha} + l_x^\alpha\dfrac{y-y^\alpha}{(a^\alpha)^2} - l_y^\alpha\dfrac{x-x^\alpha}{(a^\alpha)^2} + \tfrac{1}{2}p^\alpha\left(1 - \dfrac{|\boldsymbol{x}-\boldsymbol{x}^\alpha|^2}{(a^\alpha)^2}\right)\right) & \\ \qquad\qquad\qquad\qquad\qquad\qquad\qquad\qquad \text{if} \quad |\boldsymbol{x}-\boldsymbol{x}^\alpha| \leqslant a^\alpha. & \end{cases} \tag{5}$$

In the solution outside Γ^α all the terms are singular at $\boldsymbol{x}^\alpha$. Inside Γ^α the solution consists of a constant velocity (the first term), simple uniform shear (second and third terms), and a parabolic field (the last term). On Γ^α itself the inside and outside solutions match exactly. These different field contributions are illustrated in figure 1(*b*). The coefficients

$$\boldsymbol{F}^\alpha = (f^\alpha, l_x^\alpha, l_y^\alpha, p^\alpha) \tag{6}$$

are moments of force associated with Γ^α: f^α is the total force per unit length applied on Γ^α, l_x^α and l_y^α are the applied couples per unit length and p^α is the total force per unit length in the interior of Γ^α due to the pressure gradient,

$$p^\alpha = -\pi(a^\alpha)^2\frac{\partial P}{\partial z}. \tag{7}$$

Also, ρ is a constant arbitrary radius that must be introduced to make the velocity field determinate. It is easy to show that $\boldsymbol{U}^\alpha$ and $\boldsymbol{F}^\alpha$ are energy dissipation conjugate.

Now consider a set of N circular curves Γ^α, as illustrated in figure 2, each having a centre at $\boldsymbol{x}^\alpha$ and a radius a^α. The many-body solution is obtained by adding up the fields due to all the $4N$ forces and couples considered:

$$v(\boldsymbol{x}) = \sum_{\alpha=1}^{N} v_{(\alpha)}(\boldsymbol{x}). \tag{8}$$

This velocity field is defined everywhere. It is smooth and continuous and satisfies Poisson's equations exactly everywhere except on Γ, where it is generally discontinuous, i.e. slips. This solution should be combined with a self-equilibrium condition, stating that the sum of forces and the sum of couples must vanish, to ensure that the velocity field is steady.

It remains to determine the resultant velocities $\boldsymbol{U}^\alpha$ of each Γ^α so as to satisfy

approximately a no-slip condition on the cylinder surfaces. To do this we separate $\boldsymbol{U}^\alpha$ into four contributions; one due to $\boldsymbol{F}^\alpha$ itself, one due to other Γ that are completely separate from $\boldsymbol{x}^\alpha$, one due to any Γ enclosing $\boldsymbol{x}^\alpha$ and one due to the Γ enclosed by Γ^α:

$$\boldsymbol{U}^\alpha = \sum_{\beta=1}^{N} \boldsymbol{U}^\alpha_{(\beta)} = \boldsymbol{U}^\alpha_{(\alpha)} + \sum_{\substack{|\boldsymbol{x}^\beta-\boldsymbol{x}^\alpha| \\ >a^\beta+a^\alpha}} \boldsymbol{U}^\alpha_{(\beta)} + \sum_{\substack{|\boldsymbol{x}^\beta-\boldsymbol{x}^\alpha| \\ <a^\beta-a^\alpha}} \boldsymbol{U}^\alpha_{(\beta)} + \sum_{\substack{|\boldsymbol{x}^\alpha-\boldsymbol{x}^\beta| \\ <a^\alpha-a^\beta}} \boldsymbol{U}^\alpha_{(\beta)}. \tag{9}$$

For the first set, $\boldsymbol{U}^\alpha_{(\alpha)}$, of cylinder velocities there is only one that matches the field $v_{(\alpha)}$ exactly:

$$u^\alpha_{(\alpha)} = \frac{f^\alpha + p^\alpha}{2\pi\mu} \ln \frac{\rho}{a^\alpha}, \tag{10}$$

$$\omega^\alpha_{x(\alpha)} = \frac{l^\alpha_x}{2\pi\mu} \frac{1}{(a^\alpha)^2}, \tag{11}$$

$$\omega^\alpha_{y(\alpha)} = \frac{l^\alpha_y}{2\pi\mu} \frac{1}{(a^\alpha)^2}, \tag{12}$$

$$\bar{v}^\alpha_{(\alpha)} = \frac{1}{2\pi\mu}((f^\alpha + p^\alpha) \ln \frac{\rho}{a^\alpha} + \tfrac{1}{4} p^\alpha). \tag{13}$$

The second set of velocities cannot generally satisfy a no-slip condition with the remaining fields since these fields are nonlinear on Γ^α. Instead, we match them with the linearization (tangent plane) of the field about the centre, $\boldsymbol{x}^\alpha$, of Γ^α:

$$\sum_{\substack{|\boldsymbol{x}^\beta-\boldsymbol{x}^\alpha| \\ >a^\beta+a^\alpha}} u^\alpha_{(\beta)} = \sum_{\substack{|\boldsymbol{x}^\beta-\boldsymbol{x}^\alpha| \\ >a^\beta+a^\alpha}} v_{(\beta)}(\boldsymbol{x}^\alpha)$$

$$= \frac{1}{2\pi\mu} \sum_{\substack{|\boldsymbol{x}^\beta-\boldsymbol{x}^\alpha| \\ >a^\beta+a^\alpha}} \left((f^\beta + p^\beta) \ln \frac{\rho}{|\boldsymbol{x} - \boldsymbol{x}^\beta|} + l^\beta_x \frac{y^\alpha - y^\beta}{|\boldsymbol{x}^\alpha - \boldsymbol{x}^\beta|^2} - l^\beta_y \frac{x^\alpha - x^\beta}{|\boldsymbol{x}^\alpha - \boldsymbol{x}^\beta|^2} \right), \tag{14}$$

$$\sum_{\substack{|\boldsymbol{x}^\beta-\boldsymbol{x}^\alpha| \\ >a^\beta+a^\alpha}} \omega^\alpha_{(\beta)x} = \sum_{\substack{|\boldsymbol{x}^\beta-\boldsymbol{x}^\alpha| \\ >a^{\beta+a^\alpha}}} \frac{\partial}{\partial y} v_{(\beta)}(\boldsymbol{x}^\alpha)$$

$$= \frac{1}{2\pi\mu} \sum_{\substack{|\boldsymbol{x}^\beta-\boldsymbol{x}^\alpha| \\ >a^\beta+a^\alpha}} \left(-(f^\beta + p^\beta) \frac{y^\alpha - y^\beta}{|\boldsymbol{x}^\alpha - \boldsymbol{x}^\beta|^2} \right.$$

$$\left. + l^\beta_x \frac{(x^\alpha - x^\beta)^2 - (y^\alpha - y^\beta)^2}{|\boldsymbol{x}^\alpha - \boldsymbol{x}^\beta|^4} + 2 l^\beta_y \frac{(x^\alpha - x^\beta)(y^\alpha - y^\beta)}{|\boldsymbol{x}^\alpha - \boldsymbol{x}^\beta|^4} \right), \tag{15}$$

$$\sum_{\substack{|\boldsymbol{x}^\beta-\boldsymbol{x}^\alpha|\\ >a^\beta+a^\alpha}} \omega^\alpha_{(\beta)y} = -\sum_{\substack{|\boldsymbol{x}^\beta-\boldsymbol{x}^\alpha|\\ >a^\beta+a^\alpha}} \frac{\partial}{\partial x} v_{(\beta)}(\boldsymbol{x}^\alpha)$$

$$= \frac{1}{2\pi\mu} \sum_{\substack{|\boldsymbol{x}^\beta-\boldsymbol{x}^\alpha|\\ >a^\beta+a^\alpha}} \left((f^\beta + p^\beta) \frac{x^\alpha - x^\beta}{|\boldsymbol{x}^\alpha - \boldsymbol{x}^\beta|^2} + 2l^\beta_x \frac{(x^\alpha - x^\beta)(y^\alpha - y^\beta)}{|\boldsymbol{x}^\alpha - \boldsymbol{x}^\beta|^4} \right.$$

$$\left. + \; l^\beta_y \frac{(y^\alpha - y^\beta)^2 - (x^\alpha - x^\beta)^2}{|\boldsymbol{x}^\alpha - \boldsymbol{x}^\beta|^4} \right), \tag{16}$$

$$\sum_{\substack{|\boldsymbol{x}^\beta-\boldsymbol{x}^\alpha|\\ >a^\beta+a^\alpha}} \bar{v}^\alpha_{(\beta)} = \sum_{\substack{|\boldsymbol{x}^\beta-\boldsymbol{x}^\alpha|\\ >a^\beta+a^\alpha}} v_{(\beta)}(\boldsymbol{x}^\alpha)$$

$$= \frac{1}{2\pi\mu} \sum_{\substack{|\boldsymbol{x}^\beta-\boldsymbol{x}^\alpha|\\ >a^\beta+a^\alpha}} \left((f^\beta + p^\beta) \ln \frac{\rho}{|\boldsymbol{x} - \boldsymbol{x}^\beta|} + l^\beta_x \frac{y^\alpha - y^\beta}{|\boldsymbol{x}^\alpha - \boldsymbol{x}^\beta|^2} - l^\beta_y \frac{x^\alpha - x^\beta}{|\boldsymbol{x}^\alpha - \boldsymbol{x}^\beta|^2} \right). \tag{17}$$

The third set, produced by sources Γ^β completely enclosing Γ^α, is obtained from the internal part of the field (5). Although this may not be immediately evident, the inside field of (5) is linear on any circle within Γ^β, and hence satisfies the no-slip condition on Γ^α exactly:

$$\sum_{\substack{|\boldsymbol{x}^\beta-\boldsymbol{x}^\alpha|\\ <a^\beta-a^\alpha}} u^\alpha_{(\beta)} = \frac{1}{2\pi\mu} \sum_{\substack{|\boldsymbol{x}^\beta-\boldsymbol{x}^\alpha|\\ <a^\beta-a^\alpha}} \left((f^\beta + p^\beta) \ln \frac{\rho}{a^\beta} + l^\beta_x \frac{y^\alpha - y^\beta}{(a^\beta)^2} - l^\beta_y \frac{x^\alpha - x^\beta}{(a^\beta)^2} \right.$$

$$\left. + \; \tfrac{1}{2} p^\beta \left(1 - \frac{|\boldsymbol{x}^\alpha - \boldsymbol{x}^\beta|^2}{(a^\beta)^2} - \left(\frac{a^\alpha}{a^\beta} \right)^2 \right) \right), \tag{18}$$

$$\sum_{\substack{|\boldsymbol{x}^\beta-\boldsymbol{x}^\alpha|\\ <a^\beta-a^\alpha}} \omega^\alpha_{x(\beta)} = \frac{1}{2\pi\mu} \sum_{\substack{|\boldsymbol{x}^\beta-\boldsymbol{x}^\alpha|\\ <a^\beta-a^\alpha}} \left(l^\beta_x \frac{1}{(a^\beta)^2} - p^\beta \frac{y^\alpha - y^\beta}{(a^\beta)^2} \right), \tag{19}$$

$$\sum_{\substack{|\boldsymbol{x}^\beta-\boldsymbol{x}^\alpha|\\ <a^\beta-a^\alpha}} \omega^\alpha_{y(\beta)} = \frac{1}{2\pi\mu} \sum_{\substack{|\boldsymbol{x}^\beta-\boldsymbol{x}^\alpha|\\ <a^\beta-a^\alpha}} \left(l^\beta_y \frac{1}{(a^\beta)^2} + p^\beta \frac{x^\alpha - x^\beta}{(a^\beta)^2} \right), \tag{20}$$

$$\sum_{\substack{|\boldsymbol{x}^\beta-\boldsymbol{x}^\alpha|\\<a^\beta-a^\alpha}} \bar{v}^\alpha_{(\beta)} = \sum_{\substack{|\boldsymbol{x}^\beta-\boldsymbol{x}^\alpha|\\<a^\beta-a^\alpha}} \frac{1}{\pi(a^\alpha)^2}\int_{A^\alpha} v_{(\beta)}\,\mathrm{d}A$$

$$= \frac{1}{2\pi\mu}\sum_{\substack{|\boldsymbol{x}^\beta-\boldsymbol{x}^\alpha|\\<a^\beta-a^\alpha}} \left((f^\beta+p^\beta)\ln\frac{\rho}{a^\beta} + l^\beta_x\frac{y^\alpha-y^\beta}{(a^\beta)^2} - l^\beta_y\frac{x^\alpha-x^\beta}{(a^\beta)^2}\right.$$

$$\left. + \tfrac{1}{2}p^\beta\left(1-\frac{|\boldsymbol{x}^\alpha-\boldsymbol{x}^\beta|^2}{(a^\beta)^2}-\frac{1}{2}\left(\frac{a^\alpha}{a^\beta}\right)^2\right)\right). \quad (21)$$

The fourth set, due to a source Γ^β completely enclosed by Γ^α, may be omitted here for reasons of symmetry.

The solution for more than one cylinder is only approximate. The boundary condition is exactly satisfied only asymptotically in the limit when the cylinders are widely spaced; it will be shown below, however, that the error is negligible in most cases.

Substituting equations (10)–(21) into equation (9), we may write these equations in terms of a mobility matrix

$$\begin{Bmatrix} u^1\\ \vdots\\ u^N\\ \omega^1_x\\ \vdots\\ \omega^N_x\\ \omega^1_y\\ \vdots\\ \omega^N_y\\ \bar{v}^1\\ \vdots\\ \bar{v}^N \end{Bmatrix} = \frac{1}{2\pi\mu}\begin{bmatrix} \begin{bmatrix} A^{11} & A^{12} & \cdots & A^{1N}\\ A^{12} & A^{22} & & A^{2N}\\ \vdots & & & \vdots\\ A^{1N} & A^{2N} & \cdots & A^{NN} \end{bmatrix} & [D] & [E] & [H]\\ \left[\widetilde{D}\right] & [B] & [F] & [I]\\ \left[\widetilde{E}\right] & \left[\widetilde{F}\right] & [C] & [J]\\ \left[\widetilde{H}\right] & \left[\widetilde{I}\right] & \left[\widetilde{J}\right] & [G] \end{bmatrix} \begin{Bmatrix} f^1\\ \vdots\\ f^N\\ l^1_x\\ \vdots\\ l^N_x\\ l^1_y\\ \vdots\\ l^N_y\\ p^1\\ \vdots\\ p^N \end{Bmatrix}, \quad (22)$$

where the components of the mobility matrix are given in table 1 and a tilde denotes transpose. Now, we may write the mobility matrix for any set of parallel cylinders, apply $4N$ auxiliary conditions and solve for the remaining forces and velocities.

3. Annular flow

As a first example, consider the pressure-driven flow in an infinite eccentric annulus between two cylinders Γ^1 and Γ^2, illustrated in figure 3. Since all the boundaries in this problem are fixed we should prescribe the velocities $(u^1,u^2,\omega^1_y,\omega^2_y,\bar{v}^1,\bar{v}^2) = (0,0,0,0,0,V)$, where V is the superficial velocity (i.e. the flow rate divided by the cross-sectional area of Γ^2). The equation system (22) can be considerably reduced by considering the symmetries of the problem: $H^{11}=A^{11}$, $H^{22}=H^{21}=A^{12}=A^{22}$,

	$\beta = \alpha$	β, α separated	β enclosing α	β enclosed by α
$A^{\alpha\beta}$	$\ln \rho/a^\alpha$	$\ln \rho/\lvert\boldsymbol{x}^\alpha - \boldsymbol{x}^\beta\rvert$	$\ln \rho/a^\beta$	$\ln \rho/a^\alpha$
$B^{\alpha\beta}$	$(a^\alpha)^{-2}$	$\dfrac{(x^\alpha - x^\beta)^2 - (y^\alpha - y^\beta)^2}{\lvert\boldsymbol{x}^\alpha - \boldsymbol{x}^\beta\rvert^4}$	$(a^\beta)^{-2}$	$(a^\alpha)^{-2}$
$C^{\alpha\beta}$	$(a^\alpha)^{-2}$	$\dfrac{(y^\alpha - y^\beta)^2 - (x^\alpha - x^\beta)^2}{\lvert\boldsymbol{x}^\alpha - \boldsymbol{x}^\beta\rvert^4}$	$(a^\beta)^{-2}$	$(a^\alpha)^{-2}$
$D^{\alpha\beta}$	0	$(y^\alpha - y^\beta)/\lvert\boldsymbol{x}^\alpha - \boldsymbol{x}^\beta\rvert^2$	$(y^\alpha - y^\beta)/(a^\beta)^2$	0
$E^{\alpha\beta}$	0	$-(x^\alpha - x^\beta)/\lvert\boldsymbol{x}^\alpha - \boldsymbol{x}^\beta\rvert^2$	$-(x^\alpha - x^\beta)/(a^\beta)^2$	0
$F^{\alpha\beta}$	0	$2\dfrac{(x^\alpha - x^\beta)(y^\alpha - y^\beta)}{\lvert\boldsymbol{x}^\alpha - \boldsymbol{x}^\beta\rvert^4}$	0	0
$G^{\alpha\beta}$	$\ln \rho/a^\alpha + \frac{1}{4}$	$\ln \rho/\lvert\boldsymbol{x}^\alpha - \boldsymbol{x}^\beta\rvert$	$\begin{pmatrix} \frac{1}{2} + \ln \rho/a^\beta \\ -\frac{1}{2}(\lvert\boldsymbol{x}^\alpha - \boldsymbol{x}^\beta\rvert/a^\beta)^2 \\ -\frac{1}{4}(a^\alpha/a^\beta)^2 \end{pmatrix}$	$\begin{pmatrix} \frac{1}{2} + \ln \rho/a^\alpha \\ -\frac{1}{2}(\lvert\boldsymbol{x}^\beta - \boldsymbol{x}^\alpha\rvert/a^\alpha)^2 \\ -\frac{1}{4}(a^\beta/a^\alpha)^2 \end{pmatrix}$
$H^{\alpha\beta}$	$\ln \rho/a^\alpha$	$\ln \rho/\lvert\boldsymbol{x}^\alpha - \boldsymbol{x}^\beta\rvert$	$\begin{pmatrix} \frac{1}{2} + \ln \rho/a^\beta \\ -\frac{1}{2}(\lvert\boldsymbol{x}^\alpha - \boldsymbol{x}^\beta\rvert/a^\beta)^2 \\ -\frac{1}{2}(a^\alpha/a^\beta)^2 \end{pmatrix}$	$\ln \rho/a^\alpha$
$I^{\alpha\beta}$	0	$-(y^\alpha - y^\beta)/\lvert\boldsymbol{x}^\alpha - \boldsymbol{x}^\beta\rvert^2$	$-(y^\alpha - y^\beta)/(a^\beta)^2$	$(y^\alpha - y^\beta)/(a^\alpha)^2$
$J^{\alpha\beta}$	0	$(x^\alpha - x^\beta)/\lvert\boldsymbol{x}^\alpha - \boldsymbol{x}^\beta\rvert^2$	$(x^\alpha - x^\beta)/(a^\beta)^2$	$-(x^\alpha - x^\beta)/(a^\alpha)^2$

TABLE 1. Mobilities.

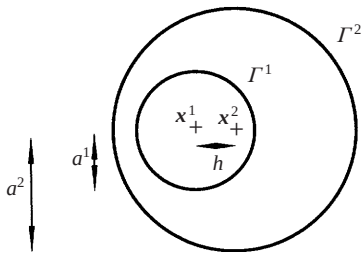

FIGURE 3. Eccentric annulus.

$J^{21} = -J^{12} = E^{12}$, $J^{11} = J^{22} = E^{21} = E^{11} = E^{22} = 0$, $C^{12} = C^{22}$, which are all deduced from table 1. Thus

$$\left.\begin{aligned} 0 &= A^{11}f^1 + A^{22}f^2 + E^{12}l_y^2 + A^{11}p^1 + H^{12}p^2, \\ 0 &= f^1 + f^2 + p^1 + p^2, \\ 0 &= C^{11}l_y^1 + C^{22}l_y^2 - E^{12}p^2, \\ 0 &= l_y^1 + l_y^2 + (E^{12}/C^{22})(f^1 + p^1), \\ 0 &= A^{11}f^1 + A^{22}f^2 + E^{12}l_y^2 + G^{11}p^1 + G^{12}p^2, \\ 2\pi\mu V &= H^{12}f^1 + A^{22}f^2 - E^{12}l_y^1 + G^{12}p^1 + G^{22}p^2. \end{aligned}\right\} \tag{23}$$

It is seen from the second and fourth of equations (23) that the system is automatically self-equilibrated. After a fair amount of algebra we obtain the solution for p^2 as

$$2\pi\mu\frac{V}{p^2} =$$

$$(G^{22}-A^{22})+\frac{G^{12}-H^{12}}{A^{11}-G^{11}}(G^{12}-A^{22})-\frac{G^{12}-A^{22}+\dfrac{G^{12}-H^{12}}{A^{11}-G^{11}}(G^{11}-A^{22})}{A^{11}-A^{22}-(C^{11}/C^{22})e}(H^{12}-A^{22})$$

$$+\left[\begin{array}{l}\dfrac{G^{12}-A^{22}+\dfrac{(G^{12}-H^{12})(G^{11}-A^{22})}{A^{11}-G^{11}}+\left(\dfrac{G^{12}-H^{12}}{A^{11}-G^{11}}\dfrac{C^{11}}{C^{22}}+1\right)(H^{12}-A^{22}-e)}{A^{11}-A^{22}-(C^{11}/C^{22})e} \\ \quad -\dfrac{G^{12}-H^{12}}{A^{11}-G^{11}}-1\end{array}\right]e, \tag{24}$$

where

$$e=\frac{(E^{12})^2}{C^{11}-C^{22}} \tag{25}$$

is a non-dimensional eccentricity parameter which vanishes in the concentric case.

Now introducing the mobilities,

$$\left.\begin{aligned} &A^{11}=\ln\frac{\rho}{a^1},\quad A^{22}=\ln\frac{\rho}{a^2},\quad C^{11}=(a^1)^{-2},\quad C^{22}=(a^2)^{-2},\\ &G^{11}=\left(\ln\frac{\rho}{a^1}+\tfrac{1}{4}\right),G^{22}=\left(\ln\frac{\rho}{a^2}+\tfrac{1}{4}\right),\\ &G^{12}=\left(\ln\frac{\rho}{a^2}+\frac{1}{2}-\frac{1}{4}\left(\frac{a^1}{a^2}\right)^2\right),\\ &H^{12}=\left(\ln\frac{\rho}{a^2}+\frac{1}{2}-\frac{1}{2}\left(\frac{a^1}{a^2}\right)^2\right),\end{aligned}\right\} \tag{26}$$

one obtains the permeability of the annulus as

$$\begin{aligned}\frac{K}{(a^1)^2}=&\frac{1}{8}\left[\left(\frac{a^2}{a^1}\right)^2+\left(\frac{a^1}{a^2}\right)^2\right]-\tfrac{1}{4}\\ &+\frac{1}{4}\frac{1-(a^1/a^2)^2(1+\ln(a^2/a^1)^2)}{\ln(a^2/a^1)^2-2(a^2/a^1)^2e}\left[1-\left(\frac{a^2}{a^1}\right)^2+2\left(\frac{a^2}{a^1}\right)^2e\right]\\ &-\frac{1}{2}\left(\left(\frac{a^2}{a^1}\right)^2-1\right)e,\end{aligned} \tag{27}$$

where

$$e=\frac{h^2}{(a^2)^2-(a^1)^2}\left(\frac{a^1}{a^2}\right)^2, \tag{28}$$

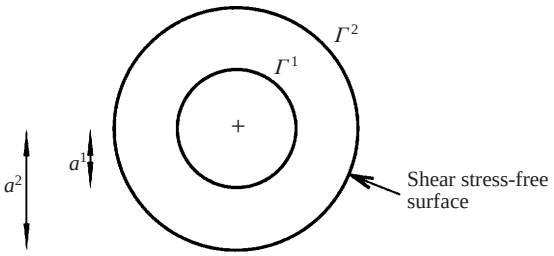

FIGURE 4. Free-surface flow.

and

$$\frac{K}{(a^1)^2} = \left(\frac{a^2}{a^1}\right)^2 \pi\mu \frac{V}{p^2} \tag{29}$$

is a non-dimensional permeability.

In fact this result is numerically indistinguishable from the exact solution, using complex variables, by Piercy, Hopper & Winny (1933):

$$\frac{K}{(a^1)^2} = \frac{1}{8}\left[\left(\frac{a^2}{a^1}\right)^2 - \left(\frac{a^1}{a^2}\right)^2\right] - \frac{1}{2}\frac{h^2F^2/(a^2)^2(a^1)^2 - h^2/(a^1)^2}{B-A}$$

$$- \left(\frac{h^2F^2}{(a^2)^2(a^1)^2} - \frac{h^2}{(a^1)^2}\right)\sum_{n=1}^{\infty}\frac{n\exp\left[-n(A+B)\right]}{\sinh n(B-A)}, \tag{30}$$

where

$$A = \tfrac{1}{2}\ln\frac{F+\sqrt{F^2+(a^2)^2}}{F-\sqrt{F^2+(a^2)^2}}, \quad B = \tfrac{1}{2}\ln\frac{F-h+\sqrt{F^2+(a^2)^2}}{F-c-\sqrt{F^2+(a^2)^2}},$$

$$F = \frac{(a^2)^2-(a^1)^2+h^2}{2h}. \tag{31}$$

The advantage of the result (27) is that it is a closed form whereas the exact solution (30) involves an infinite series.

Of course when $e = 0$, we recover the result for a concentric annulus:

$$\frac{K}{(a^1)^2} = \frac{1}{8}\left(\frac{a^2}{a^1}\right)^2 - \frac{1}{8}\left(\frac{a^1}{a^2}\right)^2 + \frac{1}{4}\frac{((a^1/a^2)^2-1)^2}{(a^1/a^2)^2\ln(a^1/a^2)^2}, \tag{32}$$

which is an exact solution.

4. Free-surface flow about a cylinder

Happel (1959) estimated the longitudinal permeability of a square array of cylinders, based on the fact that the boundary of the square unit cell is a stress-free surface. He then approximated the square cell by a circular one of the same cross-sectional area, which is a considerably simpler problem and can be solved exactly. The following example shows how to obtain Happel's result by means of the mobility method.

For the two concentric cylinders in figure 4, all couples and angular velocities vanish. Also, the system must be self-equilibrated,

$$f^1 + f^2 + p^1 + p^2 = 0, \tag{33}$$

and as no pressure gradient is applied within the rod, $p^1 = 0$. Now Happel's free-surface condition is simply expressed as

$$f^2 = 0. \tag{34}$$

The equations (22) then reduce to

$$\left.\begin{aligned} u^1 &= \frac{p^2}{2\pi\mu}(-A^{11} + H^{12}), \quad u^2 = \frac{p^2}{2\pi\mu}(-A^{12} + H^{22}), \\ \bar{v}^1 &= \frac{p^2}{2\pi\mu}(-H^{11} + G^{12}), \quad \bar{v}^2 = \frac{p^2}{2\pi\mu}(-H^{12} + G^{22}). \end{aligned}\right\} \tag{35}$$

Introducing the mobilities from table 1 (35) yields

$$\left.\begin{aligned} u^1 &= \frac{p^2}{2\pi\mu}\left(-\ln\frac{a^2}{a^1} - \frac{1}{2}\left(\frac{a^1}{a^2}\right)^2 + \frac{1}{2}\right), \quad u^2 = 0, \\ \bar{v}^1 &= \frac{p^2}{2\pi\mu}\left(-\ln\frac{a^2}{a^1} - \frac{1}{4}\left(\frac{a^1}{a^2}\right)^2 + \frac{1}{2}\right), \quad \bar{v}^2 = \frac{p^2}{2\pi\mu}\left(\frac{1}{2}\left(\frac{a^1}{a^2}\right)^2 - \frac{1}{4}\right). \end{aligned}\right\} \tag{36}$$

The superficial average fluid velocity within Γ^2 relative to the rod Γ^1 is now obtained as

$$V = (\bar{v}^2 - u^1) - (\bar{v}^1 - u^1)\left(\frac{a^1}{a^2}\right)^2 = \frac{p^2}{2\pi\mu}\left[\ln\frac{a^2}{a^1} + \left(\frac{a^1}{a^2}\right)^2 - \frac{1}{4}\left(\frac{a^1}{a^2}\right)^4 - \frac{3}{4}\right], \tag{37}$$

which may be expressed as an effective non-dimensional permeability,

$$\frac{K}{(a^1)^2} = \frac{1}{2}\left(\frac{a^2}{a^1}\right)^2 \ln\frac{a^2}{a^1} + \frac{1}{2} - \frac{1}{8}\left(\frac{a^1}{a^2}\right)^2 - \frac{3}{8}\left(\frac{a^2}{a^1}\right)^2. \tag{38}$$

This result is identical to that obtained by Happel (1959).

5. Telescopic flow

Consider the flow generated between the two cylinders in figure 3 when a purely axial motion is imposed on one cylinder relative to the other. Due to the self-equilibrium condition $f^1 + f^2 = 0$, the no-rotation condition $\omega_y^1 = \omega_y^2 = 0$ and the identities $E^{11} = E^{22} = E^{21} = 0$, $A^{12} = A^{22}$ and $C^{12} = C^{22}$, the equations reduce to

$$\left.\begin{aligned} 2\pi\mu u^1 &= (A^{11} - A^{22})f^1 + E^{12}l_y^2, \quad 2\pi\mu u^2 = 0, \\ 0 &= C^{11}l_y^1 + C^{22}l_y^2, \quad 0 = E^{12}f^1 + C^{22}(l_y^1 + l_y^2). \end{aligned}\right\} \tag{39}$$

The solution is

$$f^1 = \frac{2\pi\mu(u^1 - u^2)}{A^{11} - A^{22} + C^{11}(E^{12})^2/[(C^{22})^2 - C^{11}C^{22}]}. \tag{40}$$

Introducing the mobilities from table 1 yields

$$\xi = \frac{2\pi}{\ln(a^2/a^1) + (h/a^1)^2/[1 - (a^2/a^1)^2]}, \tag{41}$$

where ξ is a non-dimensional drag coefficient, $\xi = f^1/(u^1 - u^2)\mu$.

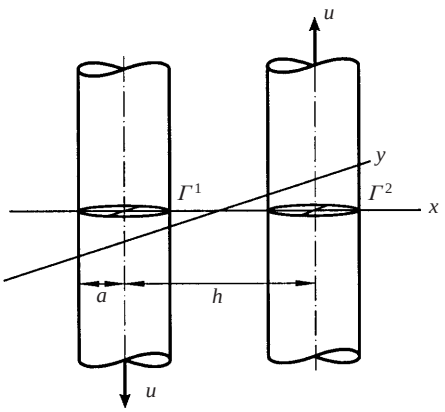

FIGURE 5. Two rods in relative motion.

In the *concentric* case, $h = 0$, equation (41) reduces to Batchelor's (1971) cell model for semi-dilute fibre suspensions,

$$\xi = \frac{2\pi}{\ln(a^2/a^1)}, \tag{42}$$

which is exact.

6. Two rods in relative motion

Consider two parallel infinite rods of equal radius a, separated by a distance h and immersed in an infinite liquid, figure 5. We seek the force f per unit length of each rod as a function of the velocity, $2u$, of one rod relative to the other.

The exact solution for the velocity field was obtained by Batchelor (1971):

$$v = -u \ln \frac{(h + \sqrt{h^2 - 4a^2})(h/2 - r\cos\theta) + r^2 - a^2}{(h - \sqrt{h^2 - 4a^2})(h/2 - r\cos\theta) + r^2 - a^2} \Big/ \ln \frac{h + \sqrt{h^2 - 4a^2}}{h - \sqrt{h^2 - 4a^2}}, \tag{43}$$

here expressed in cylindrical coordinates. It is evident that $v = -u$ on the boundary $r = a$ for any choice of a, h and θ subject to $h > 2a$. Now differentiation of (43) and integration around the boundary of one of the rods yields the force f per unit length of the rod:

$$f = \mu a \int_0^{2\pi} \frac{\mathrm{d}v}{\mathrm{d}r}(a)\,\mathrm{d}\theta = \frac{4\pi\mu u}{\ln[(h + \sqrt{h^2 - 4a^2})/(h - \sqrt{h^2 - 4a^2})]}. \tag{44}$$

For convenience we express the result in non-dimensional form, by introducing the drag coefficient $\xi = f/(2\mu u)$ and the non-dimensional spacing $H = h/2a$. Thus

$$\xi = \frac{2\pi}{\ln[(H + \sqrt{H^2 - 1})/(H - \sqrt{H^2 - 1})]}. \tag{45}$$

We now solve the same problem using the mobility method. The rods move longitudinally in opposite directions at velocities

$$u^1 = -u^2 = u \tag{46}$$

without rotating,

$$\omega_y^1 = \omega_y^2 = 0. \tag{47}$$

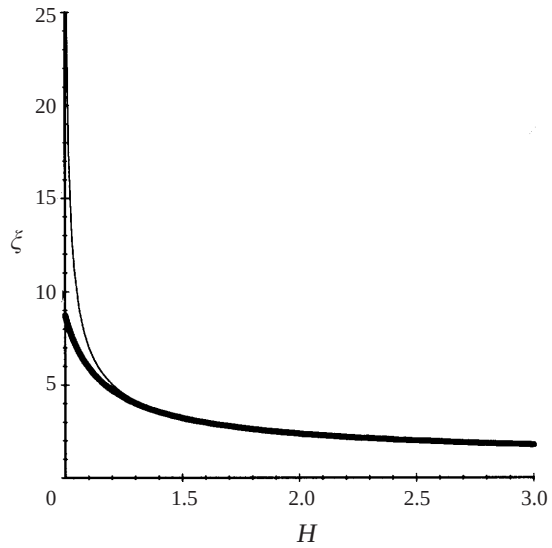

FIGURE 6. Drag coefficient ξ vs. rod spacing H for two rods, mobility solution (thick line) and exact solution (thin line).

It then follows from the symmetry that

$$f^1 = -f^2 = f, \quad -l_y^1 = -l_y^2 = l. \tag{48}$$

Note that the couples are not self-equilibrated in this case; the remaining couple simply acts on the 'container', or gives rise to an inertial flow far away, but it does not affect the drag force between the two rods. Because of the above symmetries and the fact that $E^{11} = E^{22} = 0$, equations (22) reduce to

$$2\pi\mu u = (A^{11} - A^{12})f - E^{12}l, \quad 0 = E^{12}f - (C^{11} + C^{12})l, \tag{49}$$

which yield

$$f = \frac{2\pi\mu u}{(A^{11} - A^{12}) - [(E^{12})^2/(C^{11} + C^{12})]}, \quad l = f\frac{E^{12}}{C^{11} + C^{12}}. \tag{50}$$

With the mobilities from table 1 we obtain, in non-dimensional form,

$$\xi = \frac{\pi}{\ln 2H - [1/(4H^2 - 1)]}. \tag{51}$$

For large spacings, H, the drag coefficient reduces to $\xi = \pi/\ln 2H$, which amounts to ignoring the couples.

We may now compare the mobility solution to the exact solution. The mobility result (51) is plotted in figure 6 (thick line) together with the exact solution (45) (thin line). The graph shows that the mobility solution is accurate within about 6% down to $H = 1.2$, i.e. a rod separation of 0.2 times the rod diameter. At such a small separation the interaction will be very close to pairwise. Hence this limitation should apply to a general many-rod problem as well.

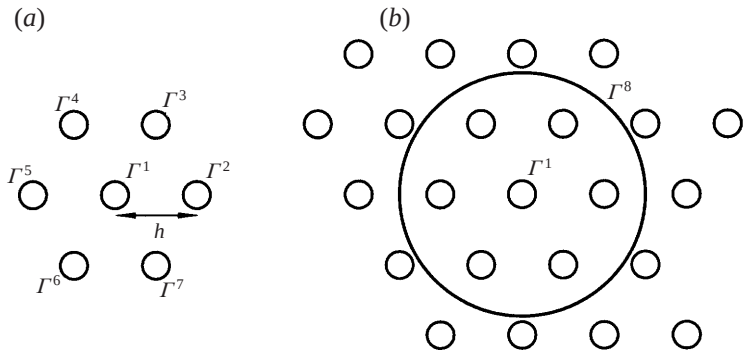

FIGURE 7. Rod moving in triangular array: (*a*) 7-cylinder model; (*b*) 8-cylinder model.

7. Rod moving in a triangular array of parallel rods

We finally consider the drag on a test rod moving relative to six stationary neighbours in a triangular array of identical rods, as illustrated in figure 7(*a*). Applying the mobility method to seven cylinders in a general arrangement leads to a 21×21 mobility matrix. This is of course rather intractable analytically. However, due to the triangular symmetry in figure 7(*a*), along with the condition that all the cylinders 2–7 perform the same motion, the mobility matrix can be reduced to 3×3:

$$\begin{Bmatrix} u^1 \\ u^2 \\ \omega_y^2 \end{Bmatrix} = \frac{1}{2\pi\mu} \begin{bmatrix} A^{11} & 6A^{12} & 6E^{12} \\ A^{21} & I & J \\ E^{12} & J & L \end{bmatrix} \begin{Bmatrix} f^1 \\ f^2 \\ l_y^2 \end{Bmatrix}, \tag{52}$$

where

$$\left.\begin{aligned} I &= A^{22} + 2(A^{23} + A^{24}) + A^{25}, \quad J = E^{22} - 2(E^{23} + E^{24}) - E^{25}, \\ L &= C^{22} + C^{23} - C^{24} - C^{25} - \sqrt{3}(F^{23} + F^{24}). \end{aligned}\right\} \tag{53}$$

In addition we apply the following constraints:

$$\omega_y^2 = 0, \quad f^1 + 6f^2 = 0. \tag{54}$$

Solving equations (52)–(54) we obtain

$$\left.\begin{aligned} f^1 &= \frac{12\pi\mu(u^1 - u^2)}{6A^{11} - 12A^{12} + I - (1/L)(6E^{12} - J)^2}, \\ l_y^2 &= -f^1 \frac{E^{12} - J/6}{L}. \end{aligned}\right\} \tag{55}$$

The mobilities are obtained from table 1:

$$\left.\begin{aligned} A^{11} &= \ln\frac{\rho}{a}, \quad A^{12} = \ln\frac{\rho}{h}, \quad E^{12} = 1/h, \\ I &= 5\ln\frac{\rho}{h} + \ln\frac{\rho}{a} - \ln 6, \quad J = \frac{5}{2h}, \quad L = \frac{1}{a^2} + \frac{35}{12h^2}. \end{aligned}\right\} \tag{56}$$

Introducing these into (55) yields

$$f^1 = \frac{12\pi\mu(u^1 - u^2)}{7\ln(h/a) - \ln 6 - \frac{49}{4}/(h^2/a^2 + 35/12)}. \tag{57}$$

The result can be expressed non-dimensionally as a drag coefficient, $\xi = f^1/\mu(u^1 - u^2)$:

$$\xi = \frac{12\pi}{7\ln 2H - \ln 6 - 49/(16H^2 + 35/3)}. \tag{58}$$

At large rod spacings or, equivalently, with couples neglected, equation (51) reduces to

$$\xi = \frac{12\pi}{7\ln 2H - \ln 6}. \tag{59}$$

We now turn to the case of an unbounded triangular array. Adding another layer of neighbouring rods, beyond the first six, would require another four equations. Although a numerical solution would present no difficulty, an analytical solution is most likely intractable. Here I choose to apply a constraint similar to that in Batchelor's cell model. By placing a rigid wall around the first layer of neighbours, as shown in figure 7(*b*), we may emulate the continuation of the array. This will answer the question of whether or not more cylinders need to be included. Owing to the way in which we have formulated the mobility method, this can be done by simply including an additional cylinder Γ^8 enclosing the other seven, as shown in figure 7(*b*). This only adds one equation to the system:

$$\begin{Bmatrix} u^1 \\ u^2 \\ u^8 \\ \omega_y^2 \end{Bmatrix} = \frac{1}{2\pi\mu} \begin{bmatrix} A^{11} & 6A^{12} & A^{18} & 6E^{12} \\ A^{21} & I & A^{28} & J \\ A^{18} & 6A^{28} & A^{88} & 6E^{82} \\ E^{12} & J & E^{82} & L \end{bmatrix} \begin{Bmatrix} f^1 \\ f^2 \\ f^8 \\ l_y^2 \end{Bmatrix}, \tag{60}$$

with

$$\omega_y^2 = 0, \quad u^2 = u^8, \quad f^1 + 6f^2 + f^8 = 0. \tag{61}$$

The equations reduce to

$$\left.\begin{aligned} 2\pi\mu u^1 &= [A^{11} - A^{12} - 6(1/L)E^{12}E^{12} + E^{12}(1/L)J]f^1 + [A^{18} - A^{12} + (1/L)JE^{12}]f^8, \\ 2\pi\mu u^2 &= [A^{12} - \tfrac{1}{6}I - (J/L)E^{12} + \tfrac{1}{6}J^2/L]f^1 + [A^{28} - \tfrac{1}{6}I + \tfrac{1}{6}J^2/L]f^8, \\ u^2 &= 0, \quad 0 = E^{12}f^1 + Jf^2 + Ll_y^2, \end{aligned}\right\} \tag{62}$$

where we have made advance use of the symmetry $A^{18} = A^{28} = A^{88}$ and the fact that $E^{82} = 0$. The solution is

$$\left.\begin{aligned} f^1 &= [2\pi\mu(u^1 - u^2)] \Bigg/ \left[A^{11} - A^{12} + E^{12}(1/L)(J - 6E^{12}) \right. \\ &\qquad \left. -(6A^{12} - 6(J/L)E^{12} - I + J^2/L)\frac{A^{18} - A^{12} + (1/L)JE^{12}}{6A^{18} - I + J^2/L}\right], \\ \frac{f^2}{f^1} &= \frac{1}{6}\left(\frac{6A^{12} - 6(J/L)E^{12} - I + J^2/L}{6A^{18} - I + J^2/L} - 1\right), \\ \frac{f^8}{f^1} &= -\frac{6A^{12} - 6(J/L)E^{12} - I + J^2/L}{6A^{18} - I + J^2/L}, \quad l_y^2 = -\frac{E^{12}}{L}f^1 - \frac{J}{L}f^2. \end{aligned}\right\} \tag{63}$$

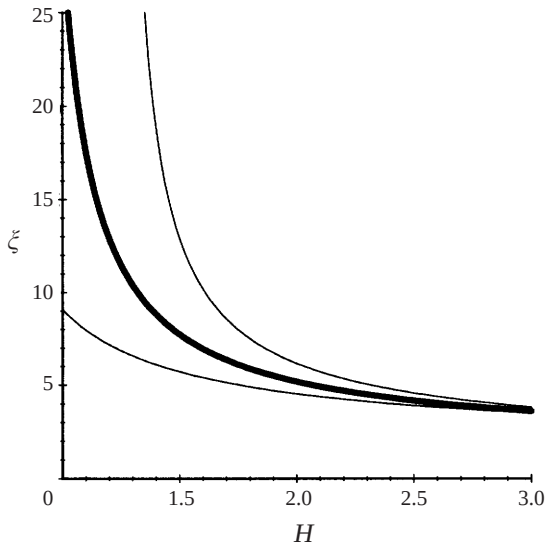

FIGURE 8. Drag coefficient ξ vs. rod spacing H for seven rods in a triangular array (thick line); Batchelor's cell-model (lower thin line); Shaqfeh & Fredrickson (upper thin line).

Introducing the mobilities (56) and, $A^{18} = A^{28} = A^{88} = \ln \rho/a^8$, we obtain

$$f^1 = 2\pi\mu(u^1 - u^2) \Bigg/ \Bigg[\ln\frac{h}{a} - \frac{7/2}{h^2/a^2 + 35/12} - \left(\ln 6 - \ln\frac{h}{a} - \frac{35/4}{h^2/a^2 + 35/12} \right) \times \frac{\ln\dfrac{a^8}{h} - \dfrac{5/2}{h^2/a^2 + 35/12}}{5\ln\dfrac{a^8}{h} + \ln\dfrac{a^8}{a} - \ln 6 - \dfrac{25/4}{h^2/a^2 + 35/12}} \Bigg]. \tag{64}$$

There is now a choice as to the radius a^8. If Γ^8 is placed far away, i.e. $a^8/h \gg h/a$, the seven-rod result (58) is recovered, as expected. For modelling purposes, the most sensible choice would be $a^8 = \sqrt{3}h$ or $a^8 = 2h$, but as I wish to prove the point that screening makes Γ^8 unnecessary, I will set $a^8 = 3h/2$, which is the most conservative thing to do without letting Γ^8 intersect the rods. This yields, in non-dimensional form,

$$\xi = 2\pi \Bigg/ \Bigg[\ln(2H) - \frac{7/2}{4H^2 + 35/12} - \left(\ln 6 - \ln(2H) - \frac{35/4}{4H^2 + 35/12} \right) \times \frac{\dfrac{5/2}{4H^2 + 35/12} - \ln\frac{3}{2}}{\dfrac{25/4}{4H^2 + 35/12} - \ln(2H) - 6\ln\frac{3}{2} + \ln 6} \Bigg]. \tag{65}$$

Now plotting equations (58) and (65) reveals that the two coincide (the thick line in figure 8). This shows that it makes no difference whether Γ^8 is included or not, so it is quite sufficient to include the first layer of neighbours when modelling an infinite

triangular array of rods. The sceptics may still want to try setting a^8 to something smaller, e.g. $a^8 = \sqrt{3}h - a$ corresponding to the smallest circle that touches the second nearest neighbour. This still makes no difference, except it behaves strangely at small h, when Γ^8 intersects the rods. The point here is that screening of the second layer of neighbours is most effective at small rod separations (screening is of course total as $H \to 1$), and (65) shows that it is as good as total at large separations, too.

We may also compare this result to the simple cell model of Batchelor,

$$\xi = \frac{2\pi}{\ln 2H}, \tag{66}$$

figure 8 (bottom thin line), or to the result of Shaqfeh & Fredrickson for aligned random rods,

$$\xi = \frac{4\pi}{\ln 2\sqrt{3}H^2/\pi + \ln\ln 2\sqrt{3}H^2/\pi + 0.1585}, \tag{67}$$

figure 8 (top thin line). The main difference between the Shaqfeh & Fredrickson theory and the present one is their neglect of fluid couples; I believe therefore that the only reason why (67) differs from (59) is that Shaqfeh & Fredrickson considered a random array rather than a triangular array.

8. Concluding remarks

The main result of this work is the mobility method for studying Stokes flow within and between cylindrical surfaces. The modelled velocity field always satisfies Poisson's equations exactly, while the approximation lies in the fluid velocity on the cylinder boundaries. The method is thus approximate in general, although it produces exact results in certain cases. It yields highly accurate or virtually exact solutions to some important problems and thus offers more accurate and more general solutions than earlier methods.

The examples elaborated here belong to either of two categories: purely pressure driven or purely shear driven. More general problems may of course involve both. For each of these categories, I chose to examine one problem that possesses an exact solution and thus serves as a test problem. The (eccentric) annular flow problem tests the method's performance for pressure-driven flows. Here its performance turns out to be perfect. The two-rod problem tests the method's performance for shear-driven flows. Here the evidence is that the singularity method is accurate for cylinder separations down to about 0.2 of a cylinder diameter, which is at least an order of magnitude less than the earlier models. For rod separations smaller than that the interaction is likely pairwise and dominated by the flow in the thinnest portion of the gap between the rods; this could be treated quite simply based on the lubrication approximation.

The most complex example brought up here is that of the drag on a test rod in a triangular array of similar rods. This illustrates the phenomenon of screening: including only the first six neighbours of the test cylinder gives the same result as including the continuation of the infinite array.

The mobility matrix was solved analytically for regular cylinder arrangements. It can of course be solved numerically, in which case general arrangements may be studied. Such a solution can deal with non-uniform cylinder diameters as well as a general lateral arrangement of the cylinders. The cylinders must not overlap, however. This method has the advantage, over for example a finite element analysis, that it

requires at most $4N$ degrees of freedom, and is therefore potentially much more powerful. Numerical analysis of general arrays using this technique should provide new insight into issues such as channelling in fibrous porous media, screening and the influence of rod arrangement and diameter distribution.

The Swedish Research Council for Engineering Sciences (TFR) is acknowledged for financing this work.

REFERENCES

Acrivos, A. & Shaqfeh, E. S. G. 1988 The effective thermal conductivity and elongational viscosity of a nondilute suspension of aligned slender rods. *Phys. Fluids* **31**, 1841.

Batchelor, G. K. 1970 Slender-body theory for particles of arbitrary cross-section in Stokes flow. *J. Fluid Mech.* **44**, 419.

Batchelor, G. K. 1971 The stress generated in a non-dilute suspension of elongated particles by pure straining motion. *J. Fluid Mech.* **46**, 813.

Brady, J. F. & Bossis, G. 1988 Stokesian Dynamics. *Ann. Rev. Fluid Mech.* **20**, 111.

Drummond, J. E. & Tahir, M. I. 1984 Laminar viscous flow through regular arrays of parallel solid cylinders. *Intl J. Multiphase Flow* **5**, 515.

Goddard, J. D. 1976 Tensile stress contribution of flow-oriented slender particles in non-Newtonian fluids. *J. Non-Newtonian Fluid Mech.* **1**, 1.

Happel, J. 1959 Viscous flow relative to arrays of cylinders. *AIChE J.* **5**, 174.

Howells, I. D. 1974 Drag due to the motion of a Newtonian fluid through a sparse random array of small fixed rigid objects. *J. Fluid Mech.* **64**, 449.

Piercy, N. A. V., Hopper, M. S. & Winny, H. F. 1933 *Phil. Mag.* **15**, 647.

Pipes, R. B. 1994 Rheological behavior of collimated fiber thermoplastic composite materials. In *Flow and Rheology in Polymer Composites Manufacturing* (ed. S. G. Advani), pp. 85–126. Elsevier.

Rayleigh, Lord 1892 On the influence of obstacles arranged in rectangular order upon the properties of a medium. *Phil. Mag.* **34**, 481.

Shaqfeh, E. S. G. & Fredrickson, G. H. 1990 The hydrodynamic stress in a suspension of rods. *Phys. Fluids* A **2**, 7.